Controlling cargo trafficking in multicomponent membranes

Tine Curk[1,2], Peter Wirnsberger[3], Jure Dobnikar[1,3], Daan Frenkel[3], Anđela Šarić[4,*]
[1]*Institute of Physics, Chinese Academy of Sciences, Beijing, China*
[2]*Department of Chemistry, University of Maribor, Maribor, Slovenia*
[3]*Department of Chemistry, University of Cambridge, Cambridge, UK*
[4]*Department of Physics and Astronomy, Institute for the Physics of Living Systems University College London, London, UK*
*

Abstract

Biological membranes typically contain a large number of different components dispersed in small concentrations in the main membrane phase, including proteins, sugars, and lipids of varying geometrical properties. Most of these components do not bind the cargo. Here, we show that such 'inert' components can be crucial for precise control of cross-membrane trafficking. Using a statistical mechanics model and molecular dynamics simulations, we demonstrate that the presence of inert membrane components of small isotropic curvatures dramatically influences cargo endocytosis, even if the total spontaneous curvature of such a membrane remains unchanged. Curved lipids, such as cholesterol, as well as asymmetrically included proteins and tethered sugars can hence all be actively participating in controlling membrane trafficking of nanoscopic cargo. We find that even a low-level expression of curved inert membrane components can determine the membrane selectivity towards the cargo size, and can be used to selectively target membranes of certain compositions. Our results suggest a robust and general way to control cargo trafficking by adjusting the membrane composition without needing to alter the concentration of receptors nor the average membrane curvature. This study indicates that cells can prepare for any trafficking event by incorporating curved inert components in either of the membrane leaflets.

Keywords: endocytosis, membrane curvature, membrane trafficking, nanoparticles, virus uptake.

Trafficking of nanoscopic cargo such as viruses and nanoparticles across biological membranes is of central interest for a wide range of phenomena, from pathogen infection, design of synthetic drug-delivery vehicles and imaging agents, to the study of nanoparticle toxicity. Trafficking of cargo that are larger than the thickness of the cell membrane typically involves tight wrapping of the object by the membrane [1, 2], followed by the membrane scission and budding off. The wrapping can be spontaneous, without any assisting factors, or supported by curvature-inducing endocytotic machinery, including BAR proteins, clathrin, and COPII [3–6].

Cellular trafficking necessarily involves crossing of physical barriers, and the physical mechanisms of nanoscopic cargo uptake have been thoroughly studied [7–9]. Much of this research has focused on understanding the physics of nanoparticle wrapping by homogeneous membranes [10–19], such as vesicles of different sizes and shapes, and highly curved membrane segments [20–24]. However, biological membranes are rarely locally homogeneous, and usually contain a large number of different components, which are present in small amounts in the main membrane phase, including lipids of different geometrical properties, embedded proteins, and anchored sugars [25]. Some of these membrane components can bind specifically to the complementary ligands on the cargo, and are referred to as receptors. Most of the membrane components, however, do not bind to the cargo, and have been thus far considered purely as spectators in the trafficking processes.

Here we show that non-cargo-binding membrane components of varying geometries can be crucial in controlling cargo trafficking. Using analytical and numerical modelling, we study the effect of small spontaneous curvatures of membrane receptors and inert lipid inclusions on the membrane uptake of

*Electronic address: a.saric@ucl.ac.uk;Telephone:+442076797295

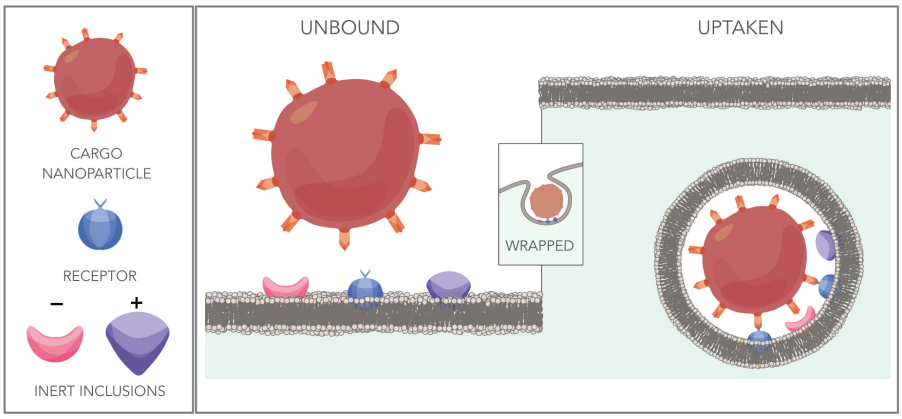

FIG. 1: **Schematic representation of the cargo-membrane system considered in this paper.** The cargo, represented as a spherical nanoparticle, is uniformly covered with ligands, which specifically bind only to receptors in the membrane (coloured in blue). In addition, inert inclusions of isotropic spontaneous positive (purple) or negative curvature (pink) can be expressed in the outer layer of the membrane at varying concentrations. Positive spontaneous curvature locally suppresses the wrapping of particles, while components with negative spontaneous curvature promote the wrapping. The cargo gets tightly wrapped by the membrane upon binding to it, and can be uptaken in a form of a bud.

nanoscopic cargo, such as nanoparticles, viruses, and other nano-objects (Figure 1). Components of small spontaneous curvatures, which are of the same order of magnitude as the curvatures of naturally occurring lipids and inclusions, can be expressed in a way that does not change the total curvature of the membrane, or cause phase-separation and formation of highly curved regions, and still substantially influence cargo uptake. We present phase diagrams showing how spontaneous curvatures of receptors and inert inclusions affect the onset of endocytosis. Importantly, we show that curved inert membrane inclusions can be used to precisely control cargo trafficking, to selectively target membranes of certain compositions, and to selectively target cargo of certain size, even if the total spontaneous curvature of the membrane remains unchanged. These findings present a robust and general way to control cargo trafficking without altering the ligand-receptor binding properties, and demonstrate that membrane trafficking depends not only on the presence of specific receptors, but also on the overall membrane composition.

We start with a theoretical analysis of the free energy cost of crossing a multicomponent membrane via passive endocytosis. We evaluate two limiting cases: when the cargo is not yet in contact with the membrane, and after endocytosis when it is fully wrapped by the membrane and detached from the parent bilayer (Figure 1). Let us consider a membrane that contains an arbitrary number of components, which can represent lipids, cargo-binding receptors, or non-interacting membrane inclusions (Figure 1). The membrane composition is completely described by a unit vector $\boldsymbol{f} = \{f_1, f_2, ...\}$ specifying the density fraction f_j of all distinct components j present in the membrane. Every membrane component j is assumed to have cylindrical symmetry with a size of the order of a transmembrane receptor and a few surrounding lipids, such that the lateral membrane area per component is $a^2 \approx 25\text{nm}^2$. Each individual component type is characterised by a spontaneous curvature $c_{0,j}$ and a favourable binding energy to the cargo $-\epsilon_j$ associated with it. Furthermore, $c_{0,j}$ is a partial molar-like quantity defined by a membrane consisting of a pure component j. The sign of the curvature is defined in Figure 1. We assume that bending modulus κ and Gaussian stiffness $\bar{\kappa}$ are the same for all components.

The total free energy change upon cargo endocytosis, ΔF, can then be written in terms of individual contributions due to the membrane curvature, ΔF_c, binding to the cargo, $\Delta\epsilon$, the mixing entropy, ΔS, and the membrane surface tension Π:

$$\Delta F = \Delta F_c + \Delta\epsilon - T\Delta S + \Pi A_{\text{w}} \,, \tag{1}$$

where T is the absolute temperature, and A_{w} is the membrane area wrapped around the cargo. The membrane curvature contribution, ΔF_c, is given by the Helfrich Hamiltonian [26]. Using the mean-field model presented in the Supplementary Information, we obtain a closed form expression for the

endocytosis free energy:

$$\Delta F = N_{\rm w} \sum_j f_j K_j \Big[\epsilon_j + \frac{2\kappa}{R_{\rm w}\rho} \left(\frac{1}{R_{\rm w}} + c_{0,j} \right) + k_{\rm B}T \ln(K_j) \Big] + \Pi A_{\rm w} + 4\pi\bar{\kappa} + N_{\rm w}\mathcal{O}\left(\frac{A_{\rm w}}{A}\right) , \tag{2}$$

where $R_{\rm w}$ is the radius of the membrane envelope wrapped around the cargo, $A_{\rm w} = 4\pi R_{\rm w}^2$ and A are the wrapped and total area of the membrane, respectively. The first term on the right-hand side captures the binding of membrane components to the cargo, the second term is the curvature penalty due to the mismatch of spontaneous curvatures, and the third term captures the effect of the membrane composition change between the flat membrane and the wrapped part with the equilibrium constant (SI):

$$K_j = \frac{e^{-\beta\left[\epsilon_j + \frac{2\kappa}{R_{\rm w}\rho}(1/R_{\rm w} + c_{0,j})\right]}}{\sum_j f_j \, e^{-\beta\left[\epsilon_j + \frac{2\kappa}{R_{\rm w}\rho}(1/R_{\rm w} + c_{0,j})\right]}} . \tag{3}$$

The prefactor $N_{\rm w} = \rho A_{\rm w} = 4\pi R_{\rm w}^2 \rho$ is the number of membrane components in the wrapped membrane, with $\rho = 1/a^2$ being the overall component number density. The fourth and fifth terms in Eq. (2) are the membrane surface tension and the Gaussian bending rigidity contribution, respectively. The latter integrates out to $4\pi\bar{\kappa}$. Finally, $\mathcal{O}(A_{\rm w}/A)$ captures all terms which can be neglected in the dilute limit. [41]

In what follows we focus on the effects of membrane composition on the passive uptake of cargo. Figure 2 shows how the endocytosis free energy changes when inert components of varying spontaneous curvatures are included into the membrane. The free energy can be shifted by several tens of $k_{\rm B}T$ even when the fraction of inert inclusions is only a few percent (solid lines in Figure 2). Inclusions of negative spontaneous curvatures (see Figure 1 for the definition) lower the free energy change for cargo uptake, while those with positive spontaneous curvature display the opposite effect. The effect of promoting endocytosis by inclusions of negative spontaneous curvature is much stronger than the corresponding suppressing effect of inclusions with positive spontaneous curvature. This asymmetry is caused by the recruitment of inclusions of desirable curvature to the wrapped part of the membrane, an effect that is similar to the recruitment of receptors that bind to the cargo.

The addition of non-interacting inclusions of spontaneous curvature can hence can be used as a mechanism to control the cargo uptake. Crucially, the effect remains even when both positive and negative inclusions are present such that the total spontaneous curvature of the multicomponent membrane is kept at zero, as displayed by dot-dashed lines in Figure 2.

To test the predictive quality of our theoretical considerations, we turn to computer simulations and explore in depth the effect of membrane composition and geometry of its components on cargo uptake. Computer simulations fully capture the possible existence of stable, partially wrapped states [12, 20, 21], which are ignored in our simple analytical model, and also allow for the analysis of the local membrane composition during the endocytotic process.

The membrane is modelled using a coarse grained one-particle thick model [27], which captures membrane fluidity and elastic properties, allows for implementation of the spontaneous curvature of individual membrane components $c_{0,j}$, and permits topological changes, such as budding (see SI). We determined the bending and the Gaussian rigidity of this membrane model to be $\kappa = -\bar{\kappa} = 22 k_{\rm B}T$ (SI) [28]. As shown in Figure S1, the membrane is composed of 'lipid' beads of zero spontaneous curvature, the cargo-binding beads which we call receptors, and inert (non-cargo binding) beads that model membrane inclusions. The fraction of receptors and inert inclusions in the membrane is given by $f_{\rm r}$ and $f_{\rm i}$. While the 'background membrane' has zero spontaneous curvature, both the receptors and inert inclusions can carry a non-zero spontaneous curvature, denoted by $c_{0,{\rm r}}$ and $c_{0,{\rm i}}$, respectively. The cargo is described as a spherical nanoparticle of a radius $R_{\rm p}$, which interacts with the membrane receptors with the interaction strength ϵ. The endocytosis is monitored through measuring the cargo wrapping by the membrane beads, $w = \sum_j w_j$, where w_j is the number of membrane beads of type j in contact with the cargo (SI).

We first consider receptors of varying spontaneous curvatures, and measure the cargo-receptor interaction energy at the onset of the cargo endocytosis, ϵ^*, as a function of the receptor curvature. Figure 3(a) shows that this onset of endocytosis can be substantially shifted if the receptors posses non-zero spontaneous curvature. The onset can be decreased by over $2k_{\rm B}T$ per receptor when going from a receptor

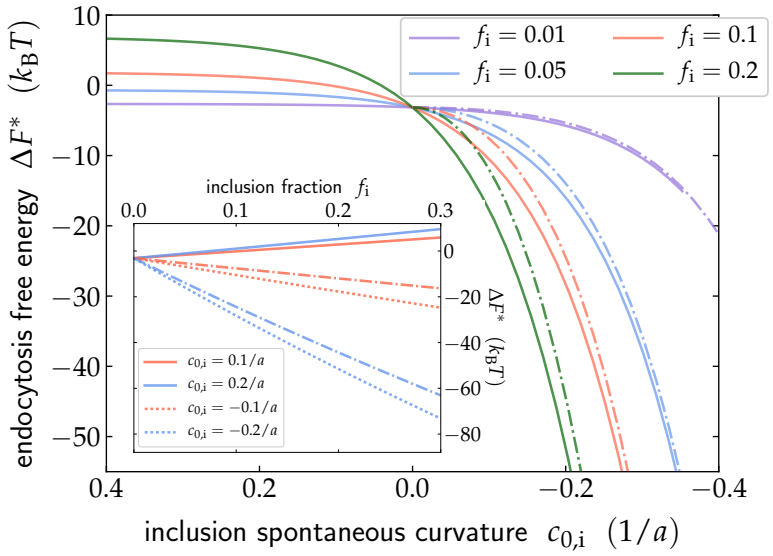

FIG. 2: **The effect of inert inclusions on the endocytosis free energy.** Changing the spontaneous curvature $c_{0,\mathrm{i}}$ of inert inclusions dramatically influences the free energy cost of crossing the membrane. The inset shows the behaviour when the fraction of inert inclusions f_i is varied at constant spontaneous curvature. The solid lines on both plots, as well dotted curves in the inset, show the case of a single inclusion type present in the membrane. The dot-dashed curves correspond to two types of inclusions with opposite spontaneous curvatures $c_{0,\mathrm{i}} = -c_{0,\mathrm{i}'}$ and $f_{\mathrm{i}'} = f_\mathrm{i}$, such that the total membrane spontaneous curvature is zero. Parameters: $R_\mathrm{w} = 5a$, $f_\mathrm{r} = 0.1$, $\epsilon_\mathrm{r} = -4k_\mathrm{B}T$, $\kappa = 23k_\mathrm{B}T$. Note that $\Delta F^* = \Delta F - 4\pi\bar{\kappa} - \Pi A_\mathrm{w}$.

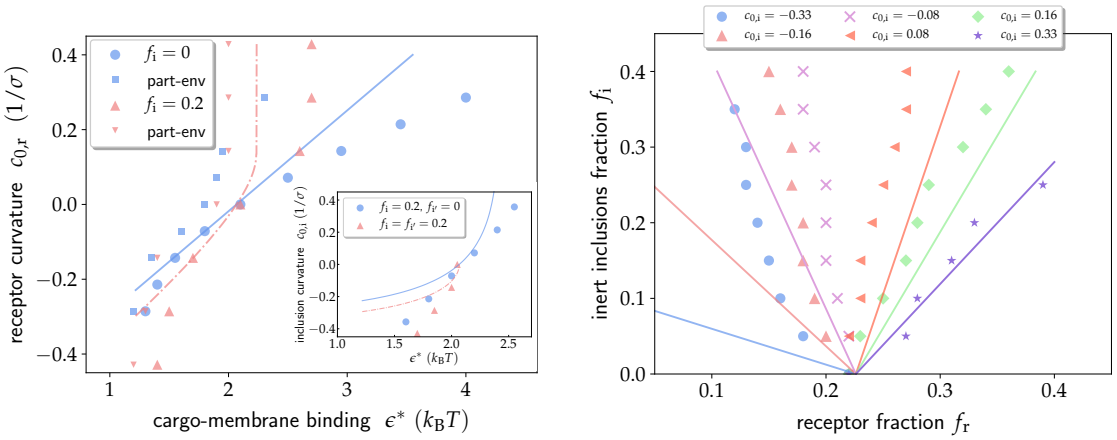

(a) (b)

FIG. 3: (a) **Spontaneous curvatures of receptors and inert inclusions control endocytosis.** Phase diagram showing the dependence of the onset of endocytosis on the receptor curvature, at constant receptor and inclusion fraction. Inset: Dependence of the onset of endocytosis on the curvature of inert inclusions at $c_{0,\mathrm{r}} = 0$. Symbols denote simulation results and lines (solid and dashed) correspond to predictions of the mean-field theory. Pink dashed lines and pink triangles show the case where the total spontaneous curvature of the membrane remains zero: $c_{0,\mathrm{i}} = -c_{0,\mathrm{r}}$ in the main plot, and two inclusion types $c_{0,\mathrm{i}'} = -c_{0,\mathrm{i}}$ in the inset. The smaller blue squares ($f_\mathrm{i} = 0$) and downward facing pink triangles ($f_\mathrm{i} = 0.2$) in the main plot show phase boundary for partial envelopment, where the degree of particle wrapping is between 10% - 20%. (b) **Tuning the onset of endocytosis by the membrane composition.** Phase diagram showing how the fraction f_r of receptor beads needed for the onset of endocytosis changes with the addition of inert beads of fraction f_i and spontaneous curvature $c_{0,\mathrm{i}}$. Receptors have zero spontaneous curvature $c_{0,\mathrm{r}} = 0$ and $\epsilon^* = 2k_\mathrm{B}T$. Solid lines show the theoretical prediction at $\Delta F = 0$. Parameters used in the analytical calculations in (a) and (b): $R_\mathrm{p} = 8\sigma$, $R_\mathrm{w} = R_\mathrm{p} + a$, $a = \sigma/\sqrt{1.21}$, $\kappa = -\bar{\kappa} = 22k_\mathrm{B}T$, $\Pi = 0$, $\epsilon_\mathrm{r} = -\epsilon^* + 1.24k_\mathrm{B}T$.

of positive spontaneous curvature ($c_{0,\mathrm{r}} = -0.16\sigma^{-1} \approx -0.03\mathrm{nm}^{-1}$) to a receptor of a negative spon-

taneous curvature ($c_{0,\mathrm{r}} = 0.16\sigma^{-1} \approx 0.03\mathrm{nm}^{-1}$) [42], Figure 3(a). This result is in line with previous analytical calculations of nanoparticle uptake by homogeneously adhesive vesicles of varying bilayer asymmetries [20].

Notably, when inert membrane inclusions are added (Figure 3(a) and the corresponding inset), be it lipids or proteins, at a constant receptor concentration, the onset of endocytosis is also significantly altered. The effect remains when both positive and negative components are present such that the total spontaneous curvature of the multicomponent membrane is kept at zero. In this case the cargo simply 'recruits' the desirable components from the membrane 'reservoir', as shown in Figure 4(b) below. Furthermore, the simulation results for the phase boundary of partially wrapped states (labeled "part-env") roughly follow the corresponding full endocytosis phase boundaries. The region between the two phase boundaries captures all states where the particle wrapping degree falls between $0.1 < w < 1$. The region is much wider for receptors with positive spontaneous curvature, than for negative spontaneous curvature, in agreement with a previous analytical study on membranes with non-zero spontaneous curvature [21].

Figure 3(b) presents a comprehensive phase diagram depicting how the addition of inert inclusions of varying spontaneous curvatures shifts the onset concentration of receptors needed for endocytosis. The ability to tune the cargo trafficking by incorporating membrane inclusions can be used as a strategy in trafficking of cargo; the level of expression of generic inclusions of a non-zero spontaneous curvature can be a way to enhance, or prevent, the endocytosis and exocytosis of nanoparticles and pathogens.

To obtain an analogous theoretical phase diagram for comparison with our simulation data, we compute the curvature $c_{0,j}(\epsilon|\Delta F = 0)$ by numerically solving Eq. (2) for a given value of receptor-cargo binding energy ϵ (Figure 3(a)), or inert inclusion fraction $f_{\mathrm{i}}(f_{\mathrm{r}}|\Delta F = 0)$ for a given value of receptor fraction f_r (Figure 3(b)), such that $\Delta F = 0$ [43] The lines in Figure 3(a) and (b) depict the results of the analytical theory, which show the same qualitative trends as the results found in simulations (symbols), although deviations can also clearly be seen. This discrepancy is mainly due to the stability of partially bound states that are not considered by the analytical theory, and the corresponding free energy barrier for the complete cargo wrapping, which can in turn delay endocytosis [44].

Biological membranes need to be highly selective when allowing for cargo trafficking, to ensure robust functioning of the cell. A hallmark of such a super-selective targeting is a sharp increase in the cargo binding upon a small change in the membrane composition. Such a behaviour results in a very low efficiency of the uptake below a threshold composition, while around the threshold the uptake sharply increases. Given that the endocytosis uptake sensitively depends on the presence of curved inclusions, it is tempting to assume that expressing such inclusions (e.g. cholesterol molecules) is one of nature's ways to tune the selectivity of membranes to specific cargo.

Here we explore the effect of inert inclusions on the selectivity of cargo uptake. We find that the sensitivity of the membrane to the cargo uptake increases with the addition of negatively curved inclusions, but decreases for positively curved inclusions (inset in Figure 4(a)). The sharpness of the transition is governed by the stability of partially wrapped states and enhanced when positively curved inclusions are present, in line with a previous analytical study [21]. Moreover, Figure 4(a) shows that the selectivity increases when inclusions with both positive and negative spontaneous curvature are added, such that the total membrane spontaneous curvature remains zero. This asymmetry arises due to recruiting of the inclusions with negative spontaneous curvature to the cargo, while inclusions with positive spontaneous curvature are expelled from the wrapped membrane area (Figure 4(b)). The effect is the same for both endocytosis and exocytosis.

A key message of these results is that for cellular trafficking it is better to create a membrane with a constant (i.e. zero) curvature from a mixture of components with opposite signs, than from homogeneous components of uniform zero curvature. Such a heterogeneous membrane is then prepared for a plethora of trafficking effects. Thus our findings suggest a generic functional role of the ubiquitous non-cargo-binding curved lipids [29–34].

In experiments, as well as in molecular dynamics simulations, what is typically probed is the amount of endocytosis in a finite time. Hence, the kinetics, and not only thermodynamics, of the cargo engulfment matters. Many experimental studies have reported the existence of an optimal size of nanoparticles for which the rate of endocytosis is the highest, while it becomes slower for lower and larger nanoparticle sizes [35, 36]. Several theoretical studies have rationalised this non-monotonic behaviour by a competition between thermodynamics, which disfavours uptake of small nanoparticles, and diffusion-limited recruitment of receptors to the cargo [11], which disfavours large nanoparticles. Similar results can be recovered by considering the competition between thermodynamic driving forces related to the creation of the bud neck and frictional forces of cargo wrapping [20]. The latter study also reported the preference

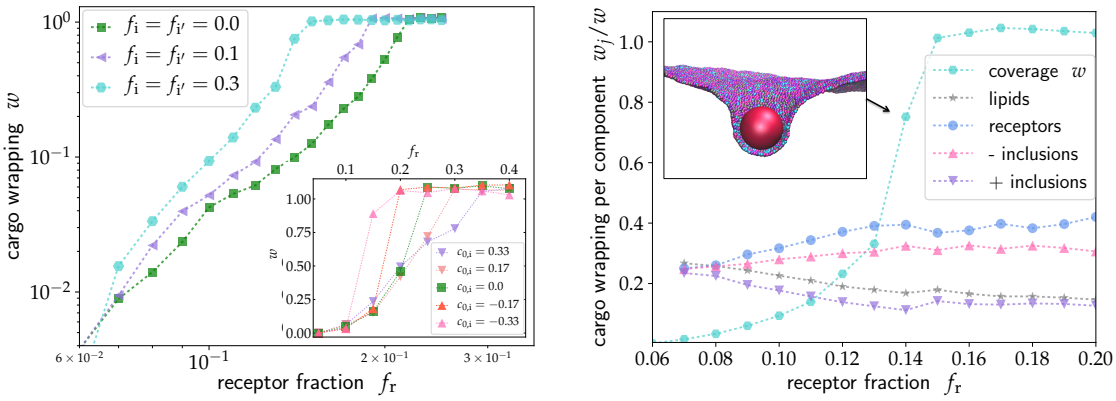

(a) (b)

FIG. 4: **Spontaneous curvatures of inert membrane components control the selectivity of cargo towards membranes of different compositions.** (a) Dependence of the cargo wrapping by the membrane on the fraction of receptors upon addition of inert beads of a certain curvature ($f_i = 0.2$, inset), or a mixture ($f_i = f_{i'}$) of inert beads of both positive and negative spontaneous curvatures $c_{0,i} = -c_{0,i'} = 0.33/\sigma$ (main figure). The coverage w above unity indicates full endocytosis. (b) The fractional coverage of the cargo particle by different membrane component types, w_j/w, at $f_i = f_{i'} = 0.3$. The cargo spontaneously recruits receptors and negatively curved inclusions, while excluding membrane 'lipid' components and positively curved inclusions. The receptor fraction is $f_r = 0.2$, the cargo nanoparticle radius is $R_p = 8\sigma$ and $\epsilon^* = 2k_BT$. Inset shows the configuration snapshot at $f_r = 0.14$, the color scheme corresponds to symbol colors used in Figure 1.

of membranes of various spontaneous curvatures towards the cargo size. When many large nanoparticles are considered, depletion of receptors can also occur [12], and the interactions between the cargo particles themselves can also significantly influence the process [37].

Here, we examine this process by explicitly measuring the rate of engulfment of nanoparticles of various sizes into multicomponent membranes. As shown in Figure 5, we recover the non-monotonic dependence of the rate of uptake on the cargo radius. Moreover, the value of the rate as well as the selectivity of the membrane uptake towards cargo of certain radii, can be altered by the presence of curved inert inclusions. Interestingly, the presence of both positively and negatively curved inert inclusions sharpens the selectivity towards the cargo size, shifting it towards the lower values. On the other hand, the presence of only positively/negatively curved inclusions decreases/increases the endocytosis rate for all cargo sizes as shown in the inset of Figure 5.

This observation can be rationalised in the following way: for large cargoes the mean curvature in the neck is positive, therefore, inclusions with positive spontaneous curvature occupy and stabilise the neck region, as shown in Figure S6. This region then presents a barrier for receptors and negatively curved inclusions to diffuse to the membrane reducing the endocytosis rate. Conversely, for small cargoes the mean curvature in the neck vanishes, and the curved inclusions do not occupy the neck region. In this case, negatively curved inclusions can freely diffuse to the membrane area that wraps the cargo, decreasing the free energy for endocytosis, and enhancing its rate (see Supplementary Information).

Our analysis shows that the presence of inert inclusions can be used not only for selecting cargo of certain membrane binding properties, but also for selecting cargo of specific sizes. This property of multicomponent membranes can be readily utilised in the design of nano-vehicles for targeted delivery of chemicals.

By considering interactions of nanoscopic cargo with multicomponent membranes, we have shown that the necessary conditions for the cargo uptake, namely the critical concentration of the membrane receptors, and the critical binding energy between the membrane receptors and the cargo ligands, can be precisely tuned by the overall membrane composition. In particular, for a given ligand-receptor pair, including only 10% of inert components of spontaneous negative curvatures, as small as 0.03nm^{-1}, can decrease the concentration of receptors needed for endocytosis by approximately 15%, enabling easier cargo uptake. Such small local spontaneous curvatures fall into the range of curvatures of typical membrane components; for instance the experimentally determined spontaneous curvature of DOPC in DOPE is $-0.05\ \text{nm}^{-1}$, while that of cholesterol is $-0.3\ \text{nm}^{-1}$ [32]. Conversely, asymmetrically expressing inert inclusions of positive spontaneous curvatures decreases endocytotic efficiency and can possibly

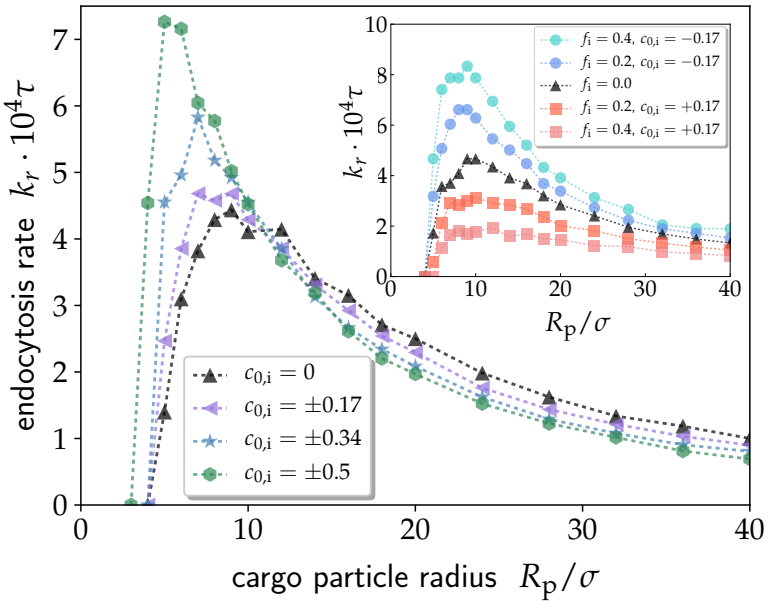

FIG. 5: **Endocytosis rate dependence on cargo size.** The presence of inert inclusions of both positive and negative spontaneous curvatures sharpens the membrane selectivity towards the cargo size. Inset: Addition of components with just negative (positive) spontaneous curvature increases (decreases) the rate. Fraction of receptor beads is fixed at $f_r = 0.4$, interaction $\epsilon^* = 2.5 k_B T$ and curvature $c_{0,r} = 0$. In the main plot the fraction of inclusions is $f_i = f_{i'} = 0.2$ with opposite spontaneous curvatures $c_{0,i} = -c_{0,i'}$. The scaling in the limit of large cargoes follows an inverse power law $k_r \sim 1/R_p^\gamma$ with the exponent $\gamma \approx 1.5$ indicating an intermediate regime between friction ($\gamma = 1$) and diffusion ($\gamma = 2$) limited endocytosis, see SI.

protect cells from entry of pathogens and other undesirable nano-objects. For comparison, common lysophospholipids exhibit positive spontaneous curvatures in the range of $0.02{-}0.25\ \mathrm{nm}^{-1}$ [33]. Therefore, the role of curved lipids, such are cholesterol, in controlling membrane physical properties possibly extends beyond adjusting the membranes fluidity and bending rigidity. Furthermore, we found that the presence of inclusions of negative spontaneous curvatures increases membrane selectivity towards the cargo nature and the cargo size (Figure 4 and Figure 5), and increases overall specificity of the trafficking processes.

Our results are in a good qualitative agreement with previous analytical calculations that considered the role of the bilayer asymmetry in controlling nanoparticle engulfment for homogeneous adhesive membranes [20]. The same study discussed their results in the context of clathrin-dependent endocytosis, where the clathrin coat effectively changes the spontaneous curvature of the membrane area wrapped around the cargo, similarly to the effect of the negatively curved receptors discussed here (Figure 3), or charged receptors discussed in [38]. Our results are also in line with a recent simulation study that shows how the phase diagram and dynamics of membrane tubulation induced by BAR domains, anisotropic membrane-curving proteins, can be modified by the presence of curved inclusions [39]. Importantly, distinct from previous studies, our results hold even if the sum of spontaneous curvatures of membrane components remains unchanged or equals to zero.

We have previously reported that the adsorption of multivalent particles onto rigid surfaces with many receptors of different binding properties can be controlled by the precise receptor composition [40]. Here we show that small concentrations of inert membrane inclusions of negative spontaneous curvature can dramatically influence the membrane selectivity towards cargo engulfment, rendering the expression of inert inclusions an attractive general mechanism for controlling cell trafficking.

Moreover, we demonstrated that the presence of negatively curved inert inclusions increases the sensitivity towards the cargo size, while the positively curved inclusions wash away this effect. Our results suggest that interactions of nano-objects with biological membranes, which are inherently inhomogeneous, display rich behaviour that goes well beyond the usually considered ligand-receptor interactions. We provide a novel and general route for modulating cargo trafficking in biological and synthetic membranes, and selectively targeting membrane composition.

Acknowledgments

We acknowledge fruitful discussions with Giuseppe Battaglia, as well as support from the Herchel Smith scholarship (T.C.), the CAS PIFI fellowship (T.C.), the UCL Institute for the Physics of Living Systems (T.C. and A.Š.), the Austrian Academy of Sciences through a DOC fellowship (P.W.), the European Union's Horizon 2020 programme under ETN grant 674979-NANOTRANS (J.D., D.F.), the Engineering and Physical Sciences Research Council (D.F. and A.Š.), the Academy of Medical Sciences and Wellcome Trust (A.Š.), and the Royal Society (A.Š.). We thank Claudia Flandoli for help with Figure 1.

References

[1] Bahrami, A. H.; Raatz, M.; Agudo-Canalejo, J.; Michel, R.; Curtis, E. M.; Hall, C. K.; Gradzielski, M.; Lipowsky, R.; Weikl, T. R. *Adv. Colloid Interface Sci.* **2014**, *208*, 214–224.
[2] Dasgupta, S.; Auth, T.; Gompper, G. *J. Phys. Condens. Matter.* **2017**, *29*, 373003–373044.
[3] Simunovic, M.; Voth, G. A.; Callan-Jones, A.; Bassereau, P. *Trends Cell Biol.* **2015**, *25*, 780–792.
[4] Johannes, L.; Parton, R. G.; Bassereau, P.; Mayor, S. *Nat. Rev. Mol. Cell Biol.* **2015**, *16*, 311–321.
[5] Johannes, L.; Wunder, C.; Bassereau, P. *Cold Spring Harb Perspect Biol.* **2014**, *6*, a016741.
[6] Simunovic, M.; Prévost, C.; Callan-Jones, A.; Bassereau, P. *Phil. Trans. R. Soc. A* **2016**, *374*, 20160034.
[7] Reynwar, B. J.; Illya, G.; Harmandaris, V. A.; Müller, M. M.; Kremer, K.; Deserno, M. *Nature* **2007**, *447*, 461–464.
[8] Zhang, S.; Gao, H.; Bao, G. *ACS Nano* **2015**, *9*, 8655–8671.
[9] Kozlov, M. M.; Weissenhorn, W.; Bassereau, P. *Lecture Notes of the Les Houches School of Physics* **2016**, *102*, 287.
[10] Lipowsky, R.; Döbereiner, H.-G. *Europhys. Lett.* **1998**, *43*, 219–225.
[11] Gao, H.; Shi, W.; Freund, L. B. *Proc. Natl. Acad. Sci. U.S.A.* **2005**, *102*, 9469–9474.
[12] Zhang, S.; Li, J.; Lykotrafitis, G.; Bao, G.; Suresh, S. *Adv. Mater.* **2009**, *21*, 419–424.
[13] Vácha, R.; Martinez-Veracoechea, F. J.; Frenkel, D. *Nano Lett.* **2011**, *11*, 5391–5395.
[14] Šarić, A.; Cacciuto, A. *Phys. Rev. Lett.* **2012**, *109*, 18810–1–18810–5.
[15] Huang, C.; Zhang, Y.; Yuan, H.; Gao, H.; Zhang, S. *Nano Lett.* **2013**, *13*, 4546–4550.
[16] Dasgupta, S.; Auth, T.; Gompper, G. *Soft Matter* **2013**, *9*, 5473–5482.
[17] Dasgupta, S.; Auth, T.; Gompper, G. *Nano Lett.* **2014**, *14*, 687–693.
[18] Schubertová, V.; Martinez-Veracoechea, F. J.; Vácha, R. *Soft Matter* **2015**, *11*, 2726–2730.
[19] Van Der Wel, C.; Vahid, A.; Šarić, A.; Idema, T.; Heinrich, D.; Kraft, D. J. *Sci. Rep.* **2016**, *6*, 32825.
[20] Agudo-Canalejo, J.; Lipowsky, R. *ACS Nano* **2015**, *9*, 3704–3720.
[21] Agudo-Canalejo, J.; Lipowsky, R. *Nano Lett.* **2015**, *15*, 7168–7173.
[22] Bahrami, A. H.; Lipowsky, R.; Weikl, T. R. *Soft Matter* **2016**, *12*, 581–587.
[23] Zhao, W.; Hanson, L.; Lou, H.-Y.; Akamatsu, M.; Chowdary, P. D.; Santoro, F.; Marks, J. R.; Grassart, A.; Drubin, D. G.; Cui, Y.; Cui, B. *Nat. Nanotechnol.* **2017**, *12*, 750–756.
[24] Yu, Q.; Othman, S.; Dasgupta, S.; Auth, T.; Gompper, G. *Nanoscale* **2018**, Advance Article.
[25] Singer, S. J.; Nicolson, G. L. *Science* **1972**, *175*, 720–731.
[26] Helfrich, W. *Z. Naturforsch. C Bio. Sci.* **1973**, *28*, 693–703.
[27] Yuan, H.; Huang, C.; Li, J.; Lykotrafitis, G.; Zhang, S. *Phys. Rev. E* **2010**, *82*, 011905–1–011905–8.
[28] Hu, M.; Briguglio, J. J.; Deserno, M. *Biophys. J.* **2012**, *102*, 1403–1410.
[29] Holopainen, J. M.; Angelova, M. I.; Kinnunen, P. K. *Biophys. J.* **2000**, *78*, 830–838.
[30] McMahon, H. T.; Gallop, J. L. *Nature* **2005**, *438*, 590–596.
[31] Roux, A.; Cuvelier, D.; Nassoy, P.; Prost, J.; Bassereau, P.; Goud, B. *EMBO J.* **2005**, *24*, 1537–1545.
[32] Martens, S.; McMahon, H. T. *Nat. Rev. Mol. Cell Biol.* **2008**, *9*, 543–556.
[33] Kamal, M. M.; Mills, D.; Grzybek, M.; Howard, J. *Proc. Natl. Acad. Sci. U.S.A.* **2009**, *106*, 22245–22250.
[34] Sorre, B.; Callan-Jones, A.; Manneville, J.-B.; Nassoy, P.; Joanny, J.-F.; Prost, J.; Goud, B.; Bassereau, P. *Proc. Natl. Acad. Sci. U.S.A.* **2009**, *106*, 5622–5626.
[35] Chithrani, B. D.; Ghazani, A. A.; Chan, W. C. *Nano Lett.* **2006**, *6*, 662–668.
[36] Jiang, W.; Kim, B. Y.; Rutka, J. T.; Chan, W. C. *Nat. Nanotechnol.* **2008**, *3*, 145–150.
[37] Chaudhuri, A.; Battaglia, G.; Golestanian, R. *Phys. Biol.* **2011**, *8*, 046002–0460011.
[38] Fošnarič, M.; Iglič, A.; Kroll, D. M.; May, S. *J. Chem. Phys.* **2009**, *131*, 105103–1–105103–9.
[39] Noguchi, H. *Soft Matter* **2017**, *13*, 7771–7779.
[40] Curk, T.; Dobnikar, J.; Frenkel, D. *Proc. Natl. Acad. Sci. U.S.A.* **2017**, 7210–7215.

[41] Note that the free energy difference (1) is related to the equilibrium ratio of the cargo densities on the two sides of the membrane: $\Delta F/k_{\mathrm{B}}T = -\ln\left(\frac{\rho_{\mathrm{cargo,in}}}{\rho_{\mathrm{cargo,out}}}\right)$. For high cargo concentrations one should use the ratio of fugacities.

[42] Assuming membrane bead size of $\sigma = 5$nm.

[43] In principle, the onset $\Delta F = -k_{\mathrm{B}}T\ln\left(\frac{\rho_{\mathrm{cargo,in}}}{\rho_{\mathrm{cargo,out}}}\right)$ is determined by the equilibrium ratio of cargo concentrations on the two sides of the membrane. Also note that $\epsilon \leq 0$ should be negative, otherwise vesicle formation is more thermodynamically stable than cargo wrapping, see SI for the discussion on membrane stability and spontaneous vesicle formation.

[44] In the mapping between simulation and analytical results, the receptor interaction is a sole fitting parameter because the theory implicitly assumes a square well-like interaction while the simulation model uses a Lennard-Jones potential. We found that $\epsilon_{\mathrm{r,theory}} = -\epsilon^*_{simulations} + 1.24k_{\mathrm{B}}T$.